ASSOCIAZIONE NAZIONALE ITALIANA DI INGEGNERIA SISMICA
ANIDIS
Italian National Association of Earthquake Engineering

XVIII CONVEGNO ANIDIS
L'ingegneria sismica in Italia
ASCOLI PICENO 2019
15-19 Settembre

Force-Based vs Displacement-Based Seismic Design of Non-structural Elements

Roberto J. Merino[a], Daniele Perrone[a], Andre Filiatrault[a,b]
[a] *University School for Advanced Studies IUSS Pavia, Piazza della Vittoria, 27100 Pavia, Italy*
[b] *State University of New York at Buffalo, Ketter Hall, 14260 Buffalo, USA*

Keywords: Non-structural elements, performance based seismic design, direct displacement-based seismic design, suspended piping restraint installations

ABSTRACT
Damage observed during past earthquakes, as well as recent loss estimation studies, have demonstrated the importance of the seismic design of non-structural elements. In a performance-based seismic design framework, the achievement of adequate performance objectives is not only related to the performance of the structure but also to the behaviour of non-structural elements. Because of lack of information on the seismic performance of non-structural elements, current seismic design provisions are either empirical in nature or based purely on judgement and lack clear definitions of performance objectives under specific seismic hazard levels. Current seismic design provisions are generally based on a force-based seismic design approach. To address these shortcomings, this paper proposes a direct displacement-based methodology for the seismic design of acceleration-sensitive non-structural elements in buildings. The proposed design procedure applies mainly to acceleration-sensitive non-structural elements suspended or anchored at a single location in the supporting structure and for which damage is the result of excessive displacements. The design of the seismic restraints for a horizontal mechanical piping system suspended from the top floor of a generic case-study four-story reinforced concrete frame building was performed both according to the proposed direct displacement-based procedure and to the force-based design procedure recently adopted in the Italian Building Code. Both design alternatives were evaluated through nonlinear time-history dynamic analyses in order to evaluate the effectiveness of the direct displacement-based design methodology as well as the influence of the design assumptions needed to perform the force-based design procedure.

1 INTRODUCTION

The performance-based seismic design of structures has advanced considerably during the last two decades. However, its application to the design of non-structural elements is largely unexplored. Recent loss estimation studies, as well as the damage observed during recent earthquakes in densely built areas, repeatedly demonstrated the importance of non-structural elements and their vulnerability even for low seismic intensities (O'Reilly et al. 2018, Perrone et al. 2018, Ercolino et al. 2012, Filiatrault et al. 2001). In comparison to structural elements and systems, there is much less information and specific guidance available on the seismic design of non-structural building elements for multiple performance levels (NIST 2018, FEMA 2012) . As a consequence the prescriptive design information currently available is based mainly on judgment and intuition rather than on scientific experimental and analytical results. Current seismic provisions distinguish between acceleration-sensitive and displacement-sensitive non-structural elements. For acceleration-sensitive non-structural elements, equivalent static design forces are specified while in the case of displacement-sensitive non-structural elements limits are imposed on the inter-storey drifts of the supporting structure (NTC 2018, CEN 2004, ASCE 2016). Non-structural building elements would benefit greatly from rational performance-based seismic design procedures. To this aim, a direct displacement-based seismic design procedure has been recently developed by Filiatrault et al. (2018). This methodology applies to acceleration-sensitive non-structural elements suspended or anchored at a single location in the supporting structure and for

which the damage is the results of excessive displacements.

This paper compares the traditional force-based seismic design approach, with special focus on the prescriptions provided by the new Italian "Norme Tecniche per le Costruzioni" (NTC), with the direct displacement-based procedure recently proposed by Filiatrault et al. (2018). The comparison was done by performing the design of the seismic restraints for a suspended horizontal mechanical piping system. The effectiveness of the two approaches was appraised thought nonlinear time history analyses.

2 FORCE-BASED SEISMIC DESIGN OF NON-STRUCTURAL ELEMENTS ACCODING TO NTC

In current European and North American design standards, the seismic design of acceleration-sensitive non-structural elements and/or its connections to the supporting structure is performed by the calculation of equivalent static design forces in the horizontal and/or vertical directions, and by applying these forces to the element's center of mass. According to the new Italian building code (NTC 2018), the horizontal static design force, F_a, can be calculated as follows:

$$F_a = \frac{S_a}{q_a} W_a \quad (1)$$

where W_a is the operating weight of the element, q_a is the behavior factor taking a value of 1.0 or 2.0 depending on the type of non-structural element, while S_a is the floor spectral acceleration. Unlike the Eurocode 8 non-structural seismic provisions, for which a simple equation is provided to calculate S_a, the new Italian standard proposes a more detailed procedure to calculate S_a from a floor response spectrum. Two methodologies are provided in order to calculate the floor response spectrum of the floor at which the non-structural elements is attached. The first methodology can be applied to all typologies of supporting structures, while the second one can only be applied to reinforced concrete (RC) moment resisting frames. In particular, in order to estimate the floor response spectrum for an RC moment resisting frame the following equations are proposed:

$$S_a(T_a) = \alpha S \left(1 + \frac{z}{H}\right) \left[\frac{a_p}{1+(a_p-1)\left(1-\frac{T_a}{aT_1}\right)^2}\right] \geq \alpha S \qquad if\ T_a < aT_1 \quad (2)$$

$$S_a(T_a) = \alpha S \left(1 + \frac{z}{H}\right) a_p \qquad if\ aT_1 \leq T_a < bT_1 \quad (3)$$

$$S_a(T_a) = \alpha S \left(1 + \frac{z}{H}\right) \left[\frac{a_p}{1+(a_p-1)\left(1-\frac{T_a}{bT_1}\right)^2}\right] \geq \alpha S \qquad if\ T_a \geq bT_1 \quad (4)$$

where:

1. α is the ratio between the peak ground acceleration for the considered location and design seismic hazard level, on soil type A, and the acceleration of gravity, g;
2. S is a coefficient that takes into account the soil type, this coefficient is provided by the code;
3. T_a is the fundamental period of the non-structural element;
4. T_1 is the fundamental period of the supporting structure in the considered direction;
5. z represents the elevation of the center of mass of the non-structural element evaluated from the foundation of the supporting structure;
6. H is the height of the building;
7. a, b and a_p are parameters defined as a function of the fundamental period of the supporting structure.

According to NTC (2018), the floor response spectra evaluated according to Equations 2 to 4 are conservative for supporting structures with a wide range of periods and also take into account the period elongation due to the nonlinear response of the supporting structure for high seismic intensities. Table 1 lists the value to be assigned to the parameters a, b and a_p depending on the fundamental period of the supporting structure.

Table 1. Parameters a, b and a_p to be used to define the floor response spectra according to NTC (2018).

	a	b	a_p
T_1 < 0.5s	0.8	1.4	5.0
0.5s<T_1<1.0s	0.3	1.2	4.0
T_1>1.0s	0.3	1.0	2.5

Once the horizontal equivalent static force has been calculated, this force should be used to design the non-structural element and its attachments to the supporting structure. A second important modification introduced in the new Italian code, with respect to Eurocode 8 (CEN 2004), concerns the definition of some rules that clarify who should be responsible for the integration of structural and non-structural designs and installations. The Italian building code distinguishes between non-structural elements built in-situ and assembled in-

situ. Examples of built in-situ non-structural elements are masonry infill panels, while examples of assembled in-situ non-structural elements are piping systems and suspended acoustic tile ceiling systems. For the non-structural elements built in-situ, it is required that the engineers/architects design the non-structural elements in accordance with the code requirements, while the construction manager must verify the correct installation of the non-structural elements and their seismic restraints. For the non-structural elements assembled in-situ, the engineers/architects should calculate the seismic demand at which the non-structural elements are subjected to for each limit state, the manufacturers should verify that their products are able to accommodate the demand provided by the designer, and the construction manager should verify the correct installation of the non-structural elements and its seismic restraints.

3 DIRECT DISPLACEMENT-BASED SEISMIC DESIGN OF NON-STRUCTURAL ELEMENTS

Filiatrault et al. (2018) recently proposed a direct displacement-based design (DDBD) procedure for the seismic design of acceleration-sensitive non-structural elements attached to a single point on the supporting structure and for which the damage occurs due to excessive displacements. Non-structural typologies for which the proposed DDBD procedure applies include piping systems (including sprinklers), cable trays, suspended ceilings, cantilevered parapets, raised access floors, anchored shelves and out-of-plane partitions, cladding and glazing. Figure 1 presents a flow chart illustrating the various steps of the direct displacement-based seismic design process for non-structural elements. These steps are discussed in this section along with a description of the information required to apply the methodology. More details on the procedure are provided in Filiatrault et al. (2018).

The first step in the design procedure is the definition of the target displacement, $\Delta_{t,a}$, or ductility, $\mu_{t,a}$, that the non-structural element should not exceed under a given seismic hazard level. This target displacement is associated with the acceptable peak deformation of the non-structural element relative to its attachment point on the supporting structure. The seismic hazard associated with the target displacement must then be defined in terms of a design floor relative displacement response spectrum. Several performance objectives could be considered simultaneously. Significant efforts have been made in recent years to develop simplified but accurate means of estimating design absolute acceleration floor response spectra (Sullivan et al. 2013, Calvi and Sullivan 2014, Calvi 2014, Vukobratović and Fajfar 2017, Merino et al. 2019). Once an absolute acceleration floor spectrum is constructed, the floor relative displacement response spectrum can be easily obtained by using the usual pseudo-spectral relationship (Filiatrault et al. 2013). In this study, the procedure developed by Merino et al. (2019) to construct consistent absolute acceleration and relative displacement floor response spectra was used.

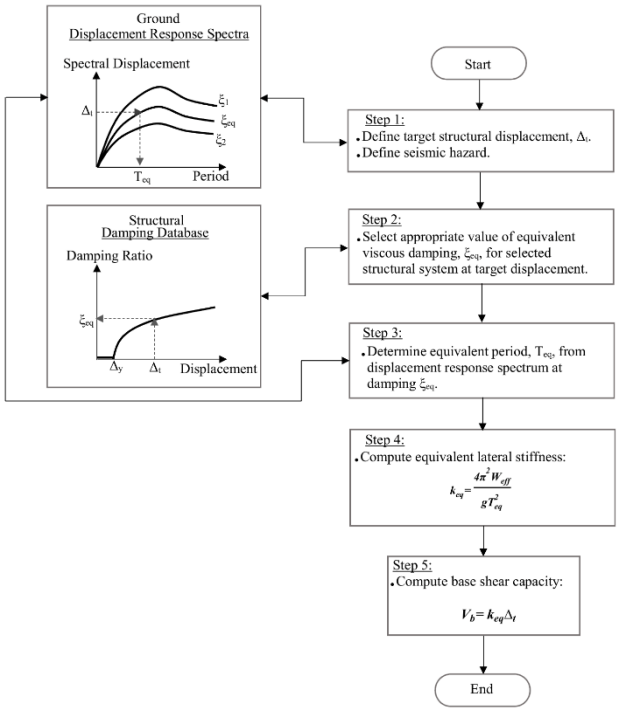

Figure 1. Flowchart of Direct Displacement-Based Seismic Design of non-structural elements (Filiatrault et al. 2018).

The second step of the DDBD procedure consists in estimating the energy dissipation characteristics of the non-structural element at the target non-structural displacement, $\Delta_{t,a}$, (or ductility $\mu_{t,a}$). This quantity is represented by an equivalent viscous damping ratio, $\xi_{eq,a}$. For this purpose, a non-structural damping database, in the form of a pre-established $\xi_{eq,a}$ - $\Delta_{t,a}$ (or $\xi_{eq,a}$ - $\mu_{t,a}$) relationship, must be established from cyclic testing data on the non-structural typology under consideration. Once this non-structural damping database has been established, $\xi_{eq,a}$ can be established using the energy-based equivalent viscous damping approach originally proposed by Jacobsen (1930, 1960).

$$\xi_{eq,a} = \frac{E_{D,\Delta_{t,a}}}{2\pi k_{eq,a}\Delta_{t,a}^2} + \xi_{i,a} \quad (5)$$

where $E_{D,\Delta t,a}$ is the energy dissipated per cycle by the non-structural element at the target displacement, $k_{eq,a}$ is the equivalent lateral stiffness of the non-structural element at the target displacement. A nominal inherent damping ratio, $\xi_{i,a}$, can also be considered to account for the energy dissipation not associated with the hysteretic response of the non-structural element.

Knowing the target displacement, $\Delta_{t,a}$, and the equivalent viscous damping ratio, $\xi_{eq,a}$, of the non-structural element at that target displacement, the equivalent (secant) period of the non-structural element, $T_{eq,a}$, can be obtained in Step 3 directly from the design floor relative displacement response spectrum derived in Step 1.

The non-structural equivalent lateral stiffness, $k_{eq,a}$, can be obtained in Step 4 as follows:

$$k_{eq,a} = \frac{4\pi^2 W_a}{g T_{eq,a}^2} \quad (6)$$

Finally, in Step 5, the resulting design force, F_a, on the non-structural element can be computed by:

$$F_a = k_{eq,a}\, \Delta_{t,a} \quad (7)$$

This design force can then be applied at the centre of mass of the non-structural element and used to design the specific bracing/anchorage components supporting the non-structural element and/or the non-structural element itself. Note that no iteration on $k_{eq,a}$ is required since the equivalent period of the non-structural element, $T_{eq,a}$, is obtained directly from the floor response spectrum at the proper damping level and that the operating weight, W_a, and damping ratio, $\xi_{eq,a}$, of the element are known at the design non-structural displacement $\Delta_{t,a}$.

4 DESIGN EXAMPLE: SUSPENDED PIPING RESTRAINT INSTALLATION

To illustrate the applications of the force-based design approach included in the most recent edition of the Italian code (NTC 2018) and of the newly proposed DDBD procedure previously described, the design of the seismic restraints for an horizontal mechanical piping system is performed. The mechanical piping system is suspended from the top floor of a generic case-study four-storey RC building located in a medium-high seismicity site in Italy (near the city of Cassino). All the details on the supporting structure, the mechanical piping system, and the results of the design calculations are provided in this section. Both design approaches then are appraised by nonlinear dynamic time-history analyses in the next section.

4.1 Case-study building

A four-storey generic case-study RC building was considered for the design example. To simplify the design, only one four-storey seismic moment resisting frame, belonging to the lateral force resisting system of the building, was designed, as shown in Figure 2. All storeys of the frame are 3.5 m in height. The frame was designed using the NTC seismic provisions (NTC 2018) with a force reduction factor q = 3.75, corresponding to a ductility class B on a assumed firm ground site near the city of Cassino, Italy with a design peak ground acceleration (with a return period of 475 years) of 0.21g. The dimensions and reinforcement details of the beams and columns are also shown in Fig. 2. The concrete strength was assumed to be 30 MPa, while the yield strength of the steel reinforcement was assumed equal to 450 MPa.

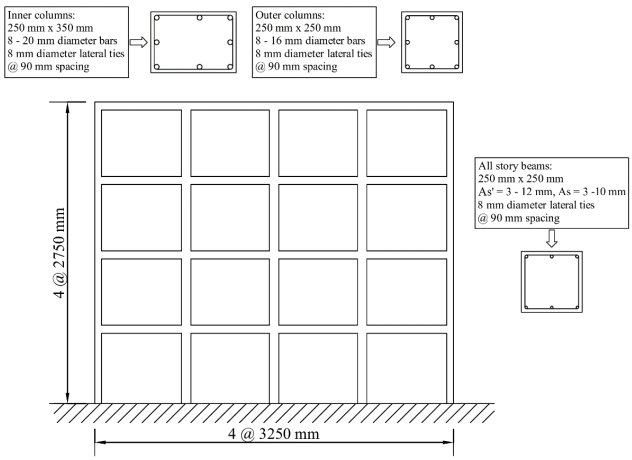

Figure 2. Case-study four-storey RC moment resisting frame.

An eigenvalue analysis of the designed frame yielded the following first three elastic natural periods based on cracked section properties: T_1 = 0.99 s, T_2 =0.29 s, and T_3 = 0.15 s.

4.2 Mechanical piping and seismic restraints properties

The mechanical piping layout selected for the design example was assumed to be part of the water supply piping system and was assumed to be suspended from the top floor of the generic case-study building described in the previous section. Figure 3 shows a plan view of the horizontal piping layout selected. The system includes three separate

pipelines: 1) a cold-water distribution line, 2) a hot-water distribution line, and 3) a hot-water recirculation line. The system includes one 18-m long main feed line connected to a perpendicular 36-m long cross main line. All pipes in the system are assumed to be made of black standard steel with a diameter of 127 mm (5 inch) along with a wall thickness of 6.5 mm. All pipe elbows and longitudinal splices are assumed rigid welded connections. The unit weight of each water filled pipe, w_a, is equal to 0.31 kN/m.

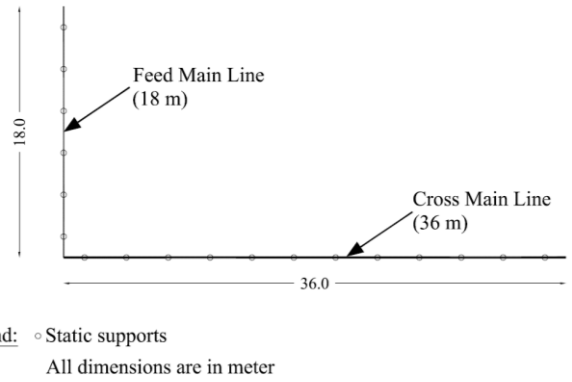

Figure 3. Case-study piping layout.

The pipes are supported by unbraced trapezes used to support vertical gravity loads only (static supports) and sway braced trapezes providing transverse or longitudinal supports. The positions of the vertical static supports are based on a standard static design considering the self-weight of the water filled pipelines. For this design example, the spacing between vertical static supports is assumed equal to 3 m. The main dimensions of the transverse and longitudinal sway braced trapezes are shown in Figure 4. For both directions, the vertical supports are provided by a horizontal channel and two vertical steel channels (all 41 mm deep) connected to the top floor slab by rail supports. The vertical channels are connected to the horizontal channel by pipe ring saddles. The transverse and longitudinal seismic restraints are provided by one and two diagonal channels, respectively. Each diagonal channel is oriented at 45° with respect to the vertical and is connected to the ends of the horizontal channel and to the ceiling slab by channel hinges.

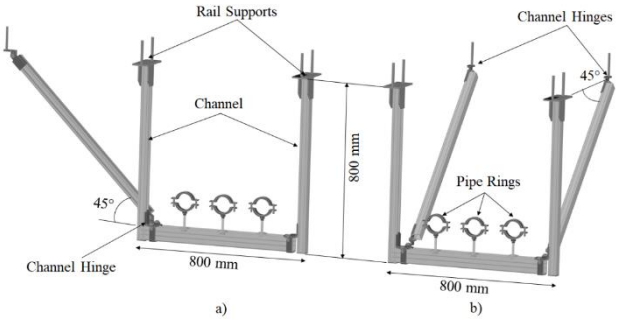

Figure 4. Configuration of the sway braced trapezes: a) Transverse, b) Longitudinal.

The design properties for the sway braced trapezes used in this design example are based on the quasi-static cyclic testing conducted by Wood et al. (2014) on standard configurations of braced trapezes. Table 2 lists the mean values of the peak strength ($F_{max,a}$), the yield displacement ($\Delta_{y,a}$) and the ductility ratio (μ_a) extracted from these test results and used for the design of the two sway braced trapeze configurations.

Table 2. Main properties of the sway braced trapeze systems based on the experimental test by Wood et al. (2014).

Direction	Mean Properties		
	$F_{max,a}$ (kN)	$\Delta_{y,a}$ (mm)	μ_a
Transverse	8.6	13.8	1.5
Longitudinal	11.9	18.2	2.5

4.3 NCT Force-Based seismic design

First, the force-based procedure included in NTC (2018) was applied to perform the seismic design of the transverse and longitudinal sway braced trapezes.

The first step in this procedure consists in the calculation of the design floor response spectrum in order to estimate S_a (Equations 2 to 4) at the fundamental period of the mechanical piping system, T_a. The following parameters were assumed to calculate the floor response spectrum at the top floor of the case-study building: α = 0.16g, S = 1.0, T_1 = 0.99s, z/H = 1.0. The parameters a, b and a_p were taken from Table 1 and are equal to 0.3, 1.2 and 4.0, respectively. Figure 4 shows the resulting design floor response spectrum evaluated according to the NTC (2018) formulation.

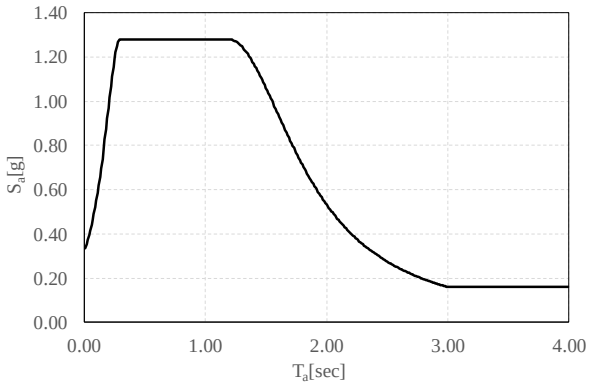

Figure 5. Design floor response spectrum evaluated according to NTC (2018).

In order to evaluate the seismic coefficient S_a in Equation 1, the fundamental period of the sway braced trapezes, T_a, must be estimated. There are significant difficulties in rationally computing natural periods of non-structural elements because of the lack of information and guidance in current building codes. In this illustrative example two assumptions were made: 1) T_a=0 representing off-resonance conditions in accordance with the current state of practice for the seismic design of piping seismic restraints (Hilti 2014); and 2) T_a=T_1 representing resonance conditions in order to conservatively maximize the value of S_a to be applied for the design of the sway braced trapezes. Once S_a is calculated, the spacing, s, between adjacent sway braced trapezes can be obtained by ensuring that the seismic demand provided by Equations 1 is less than the factored seismic capacity of each sway brace trapeze. This leads to an equation for the required spacing, s, between adjacent sway braced trapezes:

$$s \leq \frac{q_a}{\gamma_m S_a} \frac{F_{max,a}}{1.15 N_p w_a} \quad (8)$$

where γ_m is a resistance factor assumed equal to 1.25, $1.15N_pw_a$ represents the seismic mass assigned to each sway braced trapeze (W_a) in which N_p represents the number of pipes (multiplied by a factor of 1.15 to take into account the weight of the fittings and welded connections).

Table 3 summarizes the final required spacing values according to the NTC force-based design procedure for the transverse and longitudinal sway braced trapezes using a behaviour factor q_a = 2.0, as specified in NTC for suspended systems.

Table 3. Summary of NTC (2018) forced-based seismic design for transverse and longitudinal sway brace trapezes.

	T_a=0	T_a=T_1
s transverse direction	37.8 m	10.1 m
s longitudinal direction	52.4 m	13.9 m

Based on the required spacing values listed in Table 3, the required numbers of transverse and longitudinal sway braced trapezes to be installed in the feed and cross main lines were calculated, and are illustrated in Figure 6. From the data reported in Table 3 it is possible to observe wide differences in the two obtained designs depending on the assumption made for the non-structural period T_a. In particular, the value of S_a varies from 0.34g to 1.28g for T_a = 0 and T_a = T_1, respectively.

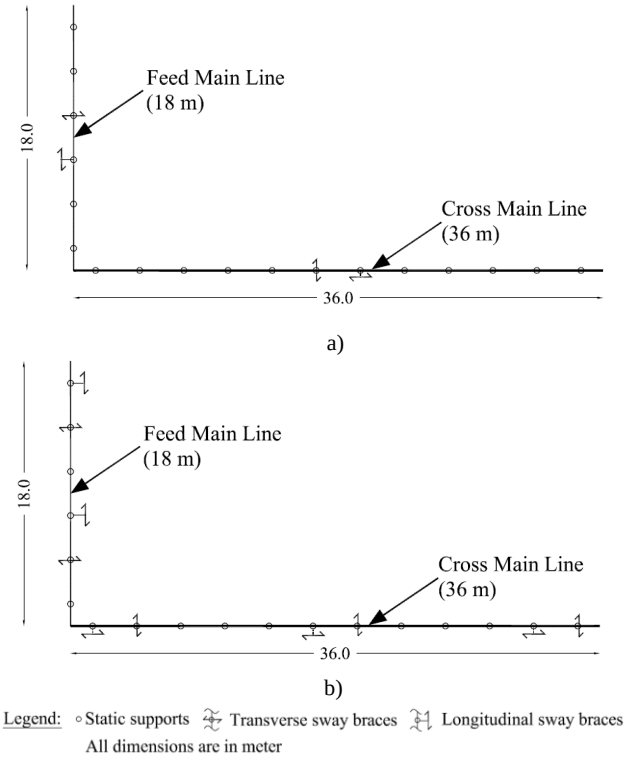

Figure 6. Resulting force-based design of sway braced trapezes according to NTC (2018): a) T_a = 0, b) T_a = T_1.

4.4 Direct Displacement-Based seismic design

In this section, the steps described in Section 3 are applied to design the transverse and longitudinal sway braced trapezes according to the DDBD procedure. The design was performed for two different performance objectives linked to different ground motion return periods: T_r = 100 and T_r = 475 years. The damage prevention performance objective, associated with T_r =100 years, is assumed to be related with a target displacement equal to the yield displacement, $\Delta_{y,a}$ of the sway braced trapezes. This performance objective is associated with a target ductility ratio equal, $\mu_{t,a}$, equal to 1.0 corresponding to target displacements of 13.8 and 18.2 mm in the longitudinal and transverse braced directions of the sway braced trapezes, respectively (Table 2). The second performance objective is associated

with life-safety limit state under design earthquakes with a return period T_r = 475 years. For this example, the life-safety prevention performance objective is associated with collapse prevention of the sway braced trapezes and is assumed to be associated with a ultimate displacement causing a 20% strength loss, $\Delta_{u,a}$, for the transverse and longitudinal directions, respectively. The associated safety prevention target ductility ratios of the sway braced trapezes are $\mu_{t,a}$ = 1.5 and 2.5 in the transverse and longitudinal braced directions, respectively (Table 2). The corresponding target displacements are 20.7 mm and 45.5 mm in the transverse and longitudinal braced directions, respectively. The required spacing, s between sway braced trapezes, s_a, can be obtained by insuring again that the seismic demand expressed by Equation 7 is less than the factored resistance of each sway braced trapeze:

$$s \leq \frac{gT_{eq,a}^2}{4\pi^2\Delta_{t,a}} \frac{F_{max,a}}{1.15\gamma_m N_p w_a} \quad (9)$$

where all the variable were previously defined. For further details on Equation 9, refer to Filiatrault et al. (2018). Based on the results by Wood et al. (2014), Filiatrault et al. (2018) developed a simple damping model that was used in this illustrative example. The resulting $\xi_{eq,a}$ - $\mu_{t,a}$ relationship can be expressed as follows:

$$\begin{aligned} \xi_{eq,a} &= 0.15 \quad \text{for } \mu_{t,a} \leq 1.0 \\ \xi_{eq,a} &= 0.18 \quad \text{for } \mu_{t,a} > 1.0 \end{aligned} \quad (10)$$

To construct the design top floor relative displacement response spectrum, S_{DF}, for the case-study building, the methodology proposed by Merino et al. (2019) was adopted. Figure 7 shows the resulting design top floor relative displacement response spectra for the case-study building. The floor response spectra are plotted for equivalent viscous damping ratios of 15% and 18% of critical according to Equation 10 for T_r = 100 years and T_r = 475 years, respectively.

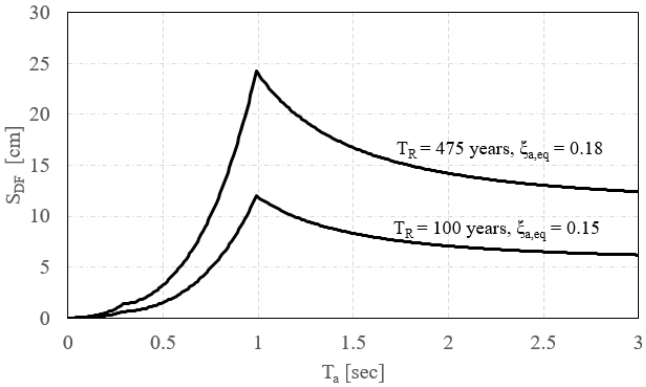

Figure 7. Top floor relative displacement response spectra according to Merino et al. (2019).

These floor relative displacement response spectra were used to complete the seismic design of the sway braced trapezes according to the DDBD procedure described in Section 3. Table 4 summarizes the results for the two considered performance objectives in terms of required spacing between adjacent sway braced trapezes, s.

Table 4. Summary of direct displacement-based seismic design for transverse and longitudinal sway brace trapezes.

	T_r =100 years	T_r=475 years
s transverse direction	27.8 m	13.6 m
s longitudinal direction	35.4 m	15.8 m

The resulting spacing of the sway braced trapezes from the direct displacement-based seismic design procedure for both the transverse and longitudinal directions is governed by the safety prevention performance objective for ground motions having a return period T_r = 475 years. Based on the governing spacing values listed in Table 4, the required numbers of transverse and longitudinal sway braced trapezes to be installed in the feed and cross main lines were calculated, and are illustrated in Figure 8.

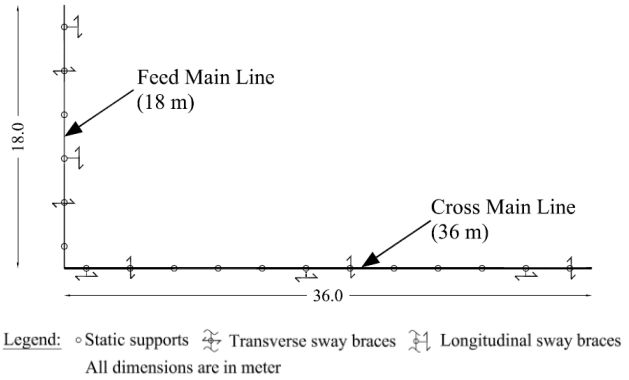

Figure 8. Resulting DDBD of sway braced trapezes according to Filiatrault et al. (2018).

5 DESIGN EXAMPLE APPRAISAL

In this section, the seismic performance of the mechanical piping systems designed according to the force-based and direct displacement-based design approaches are assessed and compared in terms of maximum displacements of the sway braced trapezes. A cascading approach was followed by performing nonlinear time history (NLTH) analyses. For this purpose, the case-study RC frames was analyzed with an ensemble of 20 ground motions to generate the floor input motions, these floor motions were then used to analyze the mechanical piping system and to evaluate the maximum displacements in the transverse and longitudinal sway braced trapezes. The analyses were performed only for T_r = 475 years because this return period governed the design.

5.1 Evaluation of the seismic demand

A set of 20 ground motions representative of the seismicity at the site of the case-study building was selected from the PEER NGA-West database (PEER 2018). In this study, a site close to the city of Cassino in Italy was chosen for the ground motions selection. This site is close to the areas struck by recent earthquakes in Italy (e.g. 2009 L'Aquila Earthquake and 2016 Central Italy Earthquake). Hazard-consistent record selection was based on spectral compatibility (matching of the geometric mean) with a conditional mean spectrum according to the methodology proposed by Jayaram et al. (2011).

5.2 Numerical modelling

The numerical models were developed using the OpenSees software (Mazzoni et al. 2006). The interaction between the structural and non-structural elements was neglected in this cascading approach, which is appropriate for this design example considering the small weight of the piping system compared to the weight of the supporting structure.

For the modelling of the RC frame, a lumped plasticity approach was used when modelling the beams and columns. Fibre sections were assigned in locations of possible plastic hinges (i.e. extreme ends of the elements), while the rest of each element was modelled using elastic properties. Elastic sections were given a reduced moment of inertia in order to simulate the cracking of the concrete per CEN (2004). The fibre sections were discretized using twenty fibres along the height of each element and ten along its width. The constitutive model assumed for the steel reinforcement was the Steel01 material in Opensees (a bilinear hysteresis with hardening in the post-elastic range), while the Concrete01 (with zero tensile strength) material was used for the concrete. The material properties of the confined concrete (peak compressive strength and strain at peak strength) were determined using the recommendations given in Priestley et al. (2007), while the ultimate compressive strain was assumed as five times the compressive strain at peak strength (Mazzoni et al. 2006).

Numerical models of the different mechanical piping system designs were also developed in OpenSees. All pipes were modelled as elastic frame elements in the same horizontal plane located at a drop height of 800 mm from the top slab of the case study building. All nodes were free to deform in translations and rotations except at the locations of vertical gravity load trapezes (static supports), where the vertical translations were constrained. The longitudinal and transverse sway braced trapezes were modelled by horizontal non-linear springs in their bracing directions using the Pinching4 uniaxial material model available in OpenSees. The hysteretic properties of each Pinching4 hysteretic spring were obtained by fitting the global force-displacement relationship obtained from the quasi-static cyclic testing conducted by Wood et al. (2014).

5.3 Results

The results of the NLTH analyses are assessed in terms of cumulative distribution functions (CDFs) of peak transverse and longitudinal displacements in the sway braced trapezes for the three design alternatives (two force-based alternatives according to NTC and one DDBD alternative) considering a ground motion return period equal to T_r = 475 years (Figure 9). The empirical CDF data shown in each graph were fitted with a lognormal CDF following the procedure proposed by Baker (2015). The target displacement associated with the performance objective is indicated by a vertical dashed line in each plot. The performance objective is associated with life-safety prevention.

Comparing the force-based configuration with $T_a = T_1$ and the displacement-based configuration it is worth noting that for both cases the number and locations of the sway braced trapezes coincide

(due to the rounding up of the sway braced trapezes' number). The sway braced trapezes designed according to the NTC force-based design procedure, and assuming $T_a = 0$, fail to meet the target displacements in both directions. The median peak displacements obtained with this design procedure exceed the target displacements by 52 mm (3.5 times) and 27 mm (1.6 times) in the transverse and longitudinal directions of the sway braced trapezes, respectively. The resulting lognormal probabilities of exceedance of the target displacements are equal to about 100% and 77% for the transverse and longitudinal sway braced trapezes, respectively.

The sway braced trapezes designed according to the proposed DDBD procedure (and according to the force-based procedure assuming $T_a = T_1$), meet the target displacements in both directions. The resulting lognormal probability of exceedance of the target displacement is nearly 0% in the longitudinal direction, while in the transverse direction, which governs the design, the probability of exceedance of the target displacement is approximately 50%.

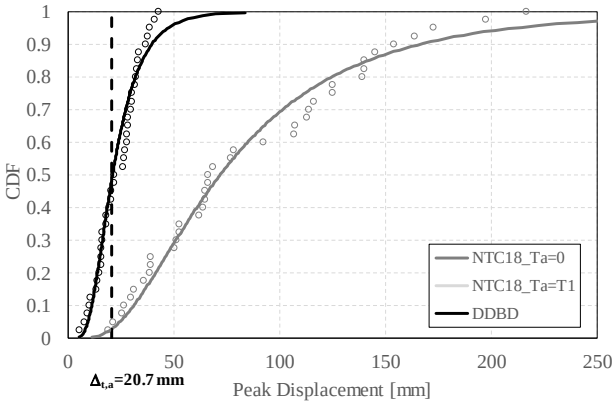

a)

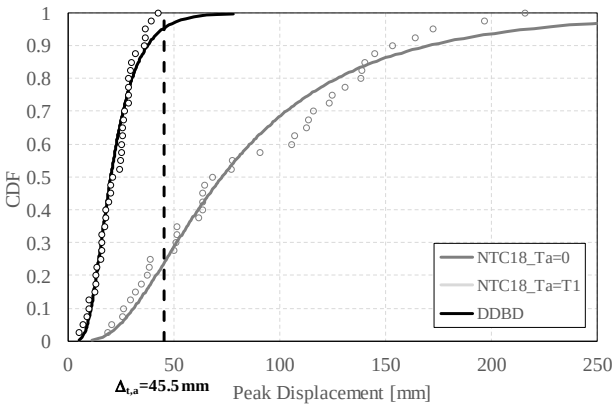

b)

Figure 9. Cumulative Distribution Functions (CDFs) for Peak Transverse and Longitudinal Displacements in Sway Braced Trapezes for NTC Design and Direct Displacement-Based Design (DDBD), T_r = 475 years, a) Transverse direction and b) Longitudinal direction.

The results demonstrate the effectiveness of the DDBD procedure. At the same time, it is observed that the calculation of the fundamental period of the non-structural element, in the force-based procedure, represents one of the most critical issues. Widely different designs are obtained depending on the what value of non-structural period is used.

The formulation adopted by NTC (2018) to evaluate the floor response spectra is also significantly affected by the fundamental period of the supporting structure. The variation of the fundamental period from 0.99 s, which is the period of the considered case-study RC frames, to a period slightly higher than 1 s implies a reduction of the floor spectral acceleration from 1.28g to 0.8g, with significant variations in the design of the sway braced trapezes system. This issue could be resolved by adopting a more accurate formulation for the definition of the floor response spectra both in terms of relative-displacements and absolute-accelerations, such as the methodology proposed by Merino et al. (2019).

The two issues above illustrate the main weaknesses of the force-based procedure for non-structural elements This issue does not occur in the DDBD procedure since the elastic periods of the non-structural element and of the supporting structure do not enter the design process.

6 CONCLUSIONS

The achievement of adequate performance objectives for non-structural elements requires the use of consistent design procedures. This paper compared the force-based procedure proposed by the most recent version of the Italian building code with a recently proposed direct displacement-based procedure. As illustrative example, the design of the sway braced trapezes for a mechanical piping system installed at the top floor of a generic case-study four-storey reinforced concrete frame was conducted using both design procedures. Both design alternatives were evaluated through non-linear time-history dynamic analyses using floor motions generated from earthquake records representative of a medium-high seismic zone in Italy. Two assumptions were made for the force-based approach, in the first case the suspended piping system was assumed to be off-resonance with the supporting structure, while in the second case the maximum amplification in the floor response

spectrum was considered assuming that the suspended piping system was in resonance with the supporting structure. Two main conclusions can be gathered from the results:

1. The direct displacement-based seismic design procedure satisfied well the performance objectives.
2. The force-based design procedure is very sensitive to the assumption made during the design. The value selected for the non-structural period could significantly modify the design the non-structural system. For the design example considered, the assumption of off-resonance between non-structural elements and the supporting structure, which is often used in practice for piping systems, leads to inadequate design, while the assumption of resonance between the supporting structure and the non-structural element leads to the same design and performance as that of the direct displacement-based procedure. Finally, it is worth noting that the fundamental period of the supporting structure could significantly affect the accuracy of the design due to the formulation proposed by the Italian code to construct floor response spectra.

ACKNOWLEDGMENTS

The work presented in this paper has been developed within the framework of the project "Dipartimenti di Eccellenza", funded by the Italian Ministry of Education, University and Research at IUSS Pavia. The authors gratefully acknowledge also the Italian Department of Civil Protection (DPC) for their financial contributions to this study through the ReLUIS 2019-2021 Project (Work Package 17 - Contributi Normativi Per Elementi Non Strutturali).

REFERENCES

ASCE, 2016. ASCE 7-16: Minimum Design Loads for Buildings and Other Structures, *American Society of Civil Engineers*, Reston, Virginia, 889 pp.

Baker, J.W., 2015. Efficient analytical fragility function fitting using dynamic structural analysis, *Earthquake Spectra*, **31**(1):579–599.

Calvi, P.M., 2014. Relative displacement floor spectra for seismic design of nonstructural elements, *Journal of Earthquake Engineering*, **18**(7), 1037-1059. DOI: 10.1080/13632469.2014.923795

Calvi, P.M. and Sullivan, T.J., 2014. Estimating floor spectra in multiple degree of freedom systems, *Earthquakes and Structures, and International Journal*, **7**(1), 17-38. DOI: 10.12989/eas.2014.7.1.017

CEN, 2004. EN-1998-1:2004: E: Eurocode 8 – Design Provisions for Earthquake Resistant Structures, *Comité Européen de Normalization*, Brussels, Belgium.

Ercolino, M., Petrone, C., Coppola, O., Magliulo, G.,2012. Report sui danni registrati a San Felice sul Panaro (Mo) in seguito agli eventi sismici del 20 e 29 maggio 2012 – v1.0, available on line: http://www.reluis.it/.

FEMA, 2012. Reducing the risks of nonstructural earthquake damage – a practical guide. FEMA E-74, Federal Emergency Management Agency and National Earthquake Hazard Reduction Program, USA.

Filiatrault, A., Uang, C.M., Folz, B., Christopoulos C., and Gatto, K., 2001. Reconnaissance report of the February 28, 2001 Nisqually (Seattle-Olympia) earthquake, *Structural Systems Research Project Report No. SSRP-2000/15*, Department of Structural Engineering, University of California, San Diego, La Jolla, CA, 62 pp.

Filiatrault, A., Tremblay, R., Christopoulos, C., Folz, B. and Pettinga, D., 2013. Elements of Earthquake Engineering and Structural Dynamics - Third Edition, *Polytechnic International Press*, Montreal, Canada, 874 pp.

Filiatrault, A., Perrone, D., Merino, R., Calvi, G.M., 2018. Performance-Based Seismic Design of Non-Structural Building Elements, *Journal of Earthquake Engineering*, https://doi.org/10.1080/13632469.2018.1512910

Hilti, 2014. Earthquake Resistant Design of Installations, Ed 1.1, Schaan, Liechtenstein, 104 p.

Jacobsen, L.S., 1930. Steady forced vibrations as influenced by damping, *ASME Transactions*, American Society of Mechanical Engineers, **52**(1): 169-181.

Jacobsen, L.S., 1960. Damping in composite structures, *Proc. of the 2nd World Conference in Earthquake Engineering*, Vol. 2, Tokyo and Kyoto, Japan, 1960, pp. 1029-1044.

Jayaram, N., Lin, T., Baker, J.W., 2011. A computationally efficient ground-motion selection algorithm for matching a target response spectrum mean and variance, *Earthquake Spectra*, **27**(3), 797-815.

Mazzoni, S., McKenna, F., Scott, M.H., Fenves, G.L., 2006. OpenSees Command language manual, *Pacific Earthquake Engineering Research Center*, Berkeley, California.

Merino Vela, R.J., Perrone, D., Filiatrault, A., 2019. Estimating consistent relative displacement and absolute acceleration floor response spectra in elastic buildings, *Proceeding Fourth International Workshop on the Seismic Performance of Non-Structural Elements*, 22-23 May 2019, Pavia, Italy, pp. 513-526, ISBN 978-88-85701-12-0, DOI 10.7414/4sponse.ID.4

NIST GCR 18-917-43, 2018. Recommendations for improved seismic performance of nonstructual elements. Applied Techonology Council, CA.

NTC, 2018. Aggiornamento delle "Norme Tecniche per le Costruzioni". Supplemento Ordinario n.8 alla Gazzetta ufficiale del 20.02.2018, Rome, Italy.

O'Reilly, G.J., Perrone, D., Fox, M., Monteiro, R., Filiatrault A., 2018. Seismic assessment and loss estimation of existing school buildings in Italy, *Engineering Structures*, **168**, 142-162, 2018.

PEER, 2018. NGA-West database, *Pacific Earthquake Engineering Research Center*, Berkeley, California, available on-line: http://peer.berkeley.edu/ngawest.

Perrone, D., Calvi, P.M., Nascimbene, R., Fischer, E. and Magliulo, G., 2018. Seismic performance and damage observation of non-structural elements during the 2016 Central Italy Earthquake, *Bulletin of Earthquake Engineering*, DOI: 10.1007/s10518-018-0361-5.

Priestley, M. J. N., Calvi, G.M., and Kowalsky, M.J., 2007. Displacement-Based Seismic Design of Structures, *IUSS Press*, Istituto Universitario di Studi Superiori di Pavia, Pavia, Italy, 721 pp.

Sullivan, T.J., Calvi, P.M. and Nascimbene, R.,2013. Towards improved floor spectra estimates for seismic design, *Earthquakes and Structures*, **4**(1), 109-132. DOI: 10.12989/eas.2013.4.1.109

Vukobratović, V. and Fajfar, P., 2017. Code-oriented floor acceleration spectra for building structures, *Bulletin of Earthquake Engineering*, **15**, 3013-3026. DOI: 10.1007/s10518-016-0076-4

Wood, R.L., Hutchinson, T.C., Hoehler, M.S., and Kreidl, B., 2014. Experimental characterization of trapeze assemblies supporting suspended non-structural systems, *Proc. of the Tenth U.S. National Conference on Earthquake Engineering*, Paper No. 905, Anchorage, Alaska, 10 p.